Human-Inspired Robot Whip Manipulation: Preparatory Actions Increase Range and Reduce Control Effort

Mahdiar Edraki[1], Silvia Buscaglione[2], Rakshith Lokesh[2]
John Peter Whitney[1], Alireza Ramezani[3], Dagmar Sternad[2,3,4]

I. INTRODUCTION

While robots have made significant progress in dexterous manipulation, most advances focus on rigid objects [1], [2]. However, real-world environments contain numerous kinds of flexible materials like ropes and fabrics, which present unique challenges due to their dynamic, underactuated nature. Conventional planning methods are challenged by these complexities and therefore often avoid dynamic interactions. This starkly contrasts with humans who excel at manipulating such objects by leveraging their natural dynamics rather than suppressing them [3], [4].

Recent machine learning approaches have attempted to address this problem, but they require extensive data and computational resources [5], [6]. Alternatively, slow quasi-static manipulation enhances stability, but fails to exploit the inherent properties of deformable objects, such as energy transfer and inertia variation [7]. However, some tasks, like flipping a rope or cracking a whip, by definition demand high-speed actions that actively exploit the object's dynamic characteristics [8], [9].

To further explore dynamic manipulation of flexible objects, we focus on whip control: a dexterous task unachievable through quasi-static control alone. Our work aims to take inspiration from humans to develop a robot controller hitting a target with a whip. Our prior experimental studies on human control of a whip revealed that humans spontaneously move and prepare the whip prior to the focal striking action to hit a target, similar to a wind-up before a throw. Such preparatory movements allow the human to set the whip's initial conditions, which significantly improved their hitting success [3] suggesting that this simplified their control of the underactuated object [10]. However, no specific evidence could be derived from these naturalistic human data.

To facilitate modeling of the control action and the whip in order to transfer insights to robot control, we modified our approach. We developed a simplified 3D-printed whip, confined to planar motion, and asked humans to execute striking actions to hit a target. Again, humans naturally incorporated preparatory counter-movements [11]. This raises a key question: What benefits do these preparatory movements have and can they be transferred to robots? This study aims to understand the benefits of this preparatory motion and how it influences the ability to successfully reach distant targets and also control effort (defined below).

To this end, we developed human-inspired simulations using a trajectory planning approach for whip control and assessed its performance on a robotic system. By generating minimum-jerk trajectories, our method replicated human motion fluidity, while enabling systematic analysis of preparatory movements. Simulations suggest that these movements extend the reachable target range, i.e., hitting success, and reduce control effort for successful execution. We validate our approach through sim-to-real experiments on a Franka Research 3 (FR3) robot moving the same 3D-printed whip.

Our results highlight the advantages of preparatory movements into dynamic manipulation tasks. By leveraging the natural dynamics of the system, rather than compensating for them, robots can achieve greater efficiency and adaptability in tasks involving flexible objects.

II. METHOD

The objective of this study was to study the strategies humans use to manipulate a 3D-printed whip to hit a target at a distance. Insights from the human experiment were then used to develop a trajectory planner to enable a robot arm to manipulate the whip and strike a distant target with its tip.

A. Human Experiment

Five volunteers (23-30 years, 4 females) were recruited to manipulate a 3D-printed whip to hit a target. Participants were naive to the task and gave informed consent using protocol #16-02-05 approved by Northeastern University. At the start of each trial, the whip was stationary with all of its links hanging down. Participants performed hand movements along the x and z axes in the sagittal plane (Fig. 1 A). Participants were instructed to perform the task with either a single striking motion or with an additional backward preparatory movement. Reflective markers were placed on the participant's shoulder, elbow, and wrist; each of the 20 whip links was marked by a small reflective patch of tape. Twelve Oqus 3+ cameras tracked the movements of the subject and the whip at a sampling frequency of 100 Hz (Qualisys, Goetheborg, Sweden) as shown in Fig. 1 B.

B. 3D-Printed Whip

The whip created in this study was constructed from 20 distinct spherical links, each individually 3D-printed with a

*This work was supported by National Institutes of Health grant R37-HD087089 and R01-CRCNS-NS120579 awarded to Dagmar Sternad, and by National Science Foundation grant FRR-2142519 awarded to Alireza Ramezani.

Departments of [1]Mechanical and Industrial Engineering, [2]Biology, [3]Electrical and Computer Engineering, and [4]Physics, Northeastern University, Boston, MA, USA [edraki.m, s.buscaglione, r.lokesh, j.whitney, a.ramezani, d.sternad]@northeastern.edu

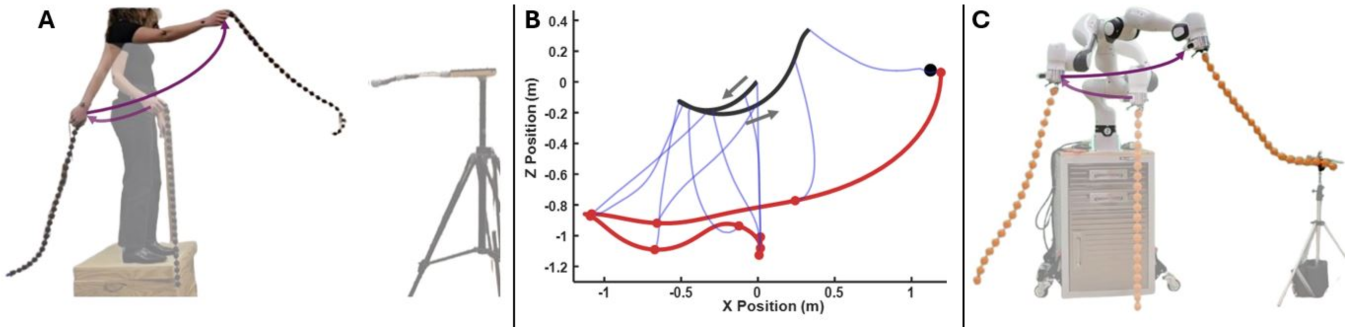

Fig. 1. **A**: Representative manipulation of the 3D-printed whip by a human participant, including the preparatory movement observed in the experiment. **B**: Kinematic trajectory of the whip handle (black) and whip tip (red) recorded using a motion capture system for the trial shown in **A**. **C**: Trajectory generated using a minimum jerk model with the human-inspired preparatory movement, implemented on the Franka robot arm to strike the target.

diameter of 50 mm and a mass of approximately 10 g. The links were connected by steel pins with a radius of 2 mm and a length of 20 mm (total length: 1 m), forming hinge joints in a serial arrangement that constrained the whip's motion to a plane.

C. Modeling the Whip Dynamics

To model the dynamics of the whip, we adopted an energy-based approach using the Euler-Lagrange formalism, expressing the system's second-order dynamics in matrix form:

$$M(q)\ddot{q} + h(q,\dot{q}) = Bu + J^{\intercal}\lambda \tag{1}$$

where B is the input matrix, derived by using the principle of virtual work. u represents the control input vector, which applies stiffness and damping at each joint using a Proportional-Derivative controller. J is the Jacobian matrix, λ is a vector of Lagrange multipliers, which constrain the handle's motion (this term contains the control effort needed to perform the task).

We assumed all links to be identical in mass, with minimal stiffness and damping. Our previous study [11] validated this model, demonstrating its effectiveness in approximating real whip dynamics, with a mean tip tracking error of less than 5 cm. This modeling approach can also accommodate whips with varying stiffness, damping, and mass (e.g., tapered whips), which we plan to use in the future.

D. Trajectory Generation

For human point-to-point movements, it has been shown that velocity exhibits a bell-shaped profile that is best approximated by a trajectory that minimizes the third derivative of position (jerk), equivalent to maximizing smoothness [12]. Equation (2) generates such a trajectory from one point to another over a given duration. We employed this equation to generate trajectories for the whip handle.

$$\begin{aligned} x(t) &= x_i + (x_f - x_i)(6\tau^5 - 15\tau^4 + 10\tau^3) \\ z(t) &= z_i + (z_f - z_i)(6\tau^5 - 15\tau^4 + 10\tau^3) \end{aligned} \tag{2}$$

$x(t)$ and $z(t)$ represent the coordinates of a linear 2D trajectory, where x_i and z_i denote the initial positions, x_f and z_f denote the final positions, and τ ($\tau = {}^{t}/_{t_f}$) is the normalized time parameter, with t_f representing the movement duration. The movement is constrained within the xz-plane, ensuring that the end-effector trajectory remains planar.

The *striking only* strategy involves a single set of x and z trajectories optimized to achieve task requirements. In contrast, the *preparing and striking* strategy consists of two sequential minimum-jerk trajectories: an initial preparatory movement followed by the main striking motion. In the *preparing and striking* approach, the endpoint of the first movement ($x_{1,f}$, $z_{1,f}$) serves as the starting position of the second movement ($x_{2,i}$, $z_{2,i}$), effectively creating a two-phase motion plan. To introduce additional flexibility for the *preparing and striking* strategy, an *overlap* parameter was introduced, allowing partial overlap between the two movements. For instance, with a 25% overlap, the velocity profile of the last 25% of the first movement was superimposed on the first 25% of the second movement for both joints. The whip handle's position was determined by integrating the summed velocity trajectory. Consequently, the *preparing and striking* strategy was defined by nine parameters: $x_{1,i}$, $z_{1,i}$, $x_{1,f}$, $z_{1,f}$, $t_{1,f}$, $x_{2,f}$, $z_{2,f}$, and $t_{2,f}$, along with the *overlap* parameter.

Similar to [11], we used a grid search optimization approach to identify optimal trajectory parameters for different target locations. MATLAB's *patternsearch* algorithm was used to identify optimal values for the hand trajectory parameters to minimize the cost function J:

$$e_i = \|\mathbf{p}_{\text{tip},i} - \mathbf{p}_{\text{target}}\|, \quad J_{\text{error}} = \min(e_i)^2 \tag{3}$$

$$J_{\text{error}} = \begin{cases} 0, & \text{if } J_{\text{error}} < 0.01^2 \\ J_{\text{error}}, & \text{otherwise} \end{cases} \tag{4}$$

$$J_{\text{effort}} = \sum_i \lambda_i^2, \quad J = \alpha J_{\text{error}} + J_{\text{effort}} \tag{5}$$

The optimization cost function was designed to balance accuracy in striking the target with control effort efficiency. The positional error at each time step, e_i, was defined as the Euclidean distance between the whip tip position $\mathbf{p}_{\text{tip},i}$ and the target position $\mathbf{p}_{\text{target}}$. To evaluate task efficiency, the cost function considers the minimum squared error over

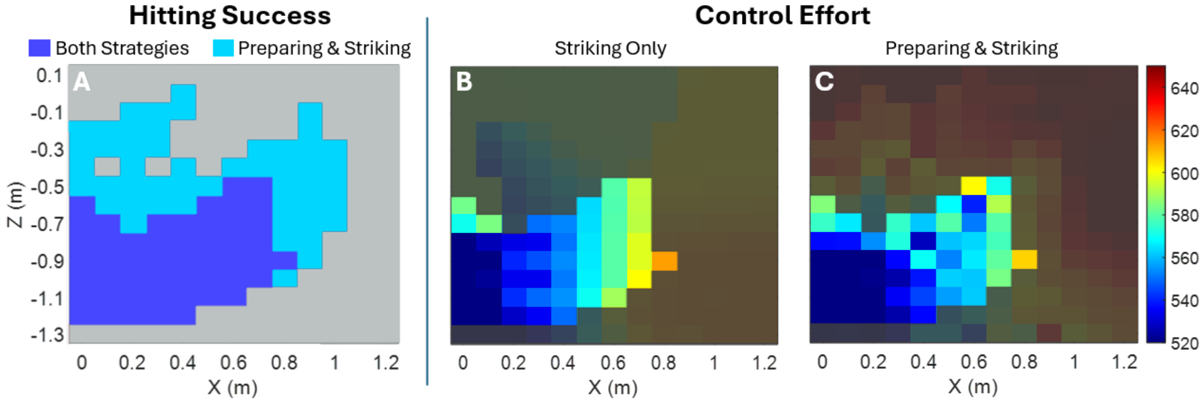

Fig. 2. **A**: Binary hit map for the two strategies. An error of less than 1cm between the whip tip and target was considered a hit (shown in blue). Farther targets were only hit with the *preparing and striking* strategy (bright blue). The control effort (in newtons) needed to manipulate the whip to hit the target with the *striking only* (**B**) and the *preparing and striking* (**C**) are masked to highlight targets where both strategies could successfully hit the target.

the trajectory, denoted as J_{error}. If the distance between the whip tip and target was less than 1 cm, it was assumed to be a successful hit, and J_{error} was set to zero. Additionally, control effort was quantified as the sum of squared control inputs over time, $J_{\text{effort}} = \sum_i \lambda_i^2$, promoting energy-efficient motions. The final objective function, J, was a weighted sum of these two terms, where α scaled the contribution of the error term, ensuring that the optimization prioritizes both accuracy and efficiency in executing the whip motion. Based on the human experiment, the bounds for the optimization parameters were -0.2 m to 0.2 m for all x and z parameters, 1 s to 2 s for the duration parameters, and 0 to 100 for the percent overlap parameter. The *patternsearch* optimizer was configured with a maximum of 200 iterations, an initial mesh size of 0.0001, and a mesh tolerance of 0.0001.

E. Robot Setup and Apparatus

The generated trajectories were tested on a 7-degree-of-freedom Franka Research 3 (FR3) robot arm (Fig. 1C), which was impedance controlled in joint space via a custom C++ program running at 1 kHz. A custom-designed passive end-plate was mounted to the robot's end effector to securely hold the whip.

III. RESULTS

In the human experiment, participants performed with two distinct strategies to complete the task: a single, direct hand movement toward the target (*striking only*) and a strategy that included an additional preparatory movement before striking (*preparing and striking*) [11]. The movements with preparation reached farther targets and more successful hits.

A similar comparison was conducted in simulation applying the optimization grid search across tested target locations for both the *striking only* and *preparing and striking* strategies. Fig. 2 A illustrates the target locations in the x-z plane that were successfully hit by each strategy. The fact that the preparatory movements hit farther targets provides one explanation for why participants may favor the more complex *preparing and striking* strategy over *striking only*.

Fig. 2 B and C depict the control effort, J_{effort} calculated in Eqn. 5, required for each strategy. Among target locations where both strategies succeeded, the *preparing and striking* strategy generally required less control effort. This suggests that, beyond extending the reachable range, participants may also prefer this strategy for its energetic efficiency.

The sim-to-real transfer of this approach is demonstrated in Fig.1 C, where the Franka robot arm was able to successfully strike the target with the whip.

IV. DISCUSSION AND CONCLUSIONS

This study explored human strategies for manipulating a 3D-printed whip to strike a target and explored features in simulation successfully implemented a modeled human trajectory on a robot. The simulations revealed that the *preparing and striking* strategy not only extended the range of reachable targets, but also reduced control effort compared to *striking only*. Since both strategies adhered to similar velocity constraints (enforced through time constraints in optimization), this suggests that the preparatory movements help energize the whip more efficiently, allowing it to reach farther and higher targets (in the z-direction). This likely stems from leveraging rather than compensating the passive dynamics of the whip. Beyond validating human-inspired motion planning, our results demonstrates the advantages of incorporating preparatory movements into robotic control strategies to achieve greater efficiency by harnessing the natural behavior of flexible objects.

By bridging human motor control with robotic motion planning, this work contributes to the development of more dexterous and adaptive robots for handling flexible materials. The insights gained extend beyond whip manipulation, with potential applications in tasks involving fabrics, liquids, and soft robotic systems, where dynamic interactions play a crucial role. Future work can further refine these strategies by integrating whips with different dynamics (e.g., a tapered whip), and by incorporating feedback control, complementing the trajectory planner.

References

[1] C. Chi, Z. Xu, S. Feng, *et al.*, *Diffusion Policy: Visuomotor Policy Learning via Action Diffusion*, arXiv:2303.04137 [cs], Mar. 2024. DOI: 10.48550/arXiv.2303.04137. [Online]. Available: http://arxiv.org/abs/2303.04137 (visited on 03/30/2025).

[2] Y. Park, J. S. Bhatia, L. Ankile, and P. Agrawal, *DexHub and DART: Towards Internet Scale Robot Data Collection*, arXiv:2411.02214 [cs], Nov. 2024. DOI: 10.48550/arXiv.2411.02214. [Online]. Available: http://arxiv.org/abs/2411.02214 (visited on 03/25/2025).

[3] A. Krotov, M. Russo, M. Nah, N. Hogan, and D. Sternad, "Motor control beyond reach—how humans hit a target with a whip," *Royal Society Open Science*, vol. 9, no. 10, p. 220 581, Oct. 2022.

[4] A. Verleysen, M. Biondina, and F. wyffels, "Video dataset of human demonstrations of folding clothing for robotic folding," *The International Journal of Robotics Research*, vol. 39, no. 9, pp. 1031–1036, Aug. 2020.

[5] C. Chi, B. Burchfiel, E. Cousineau, S. Feng, and S. Song, "Iterative Residual Policy: For Goal-Conditioned Dynamic Manipulation of Deformable Objects," in *Proceedings of RSS*, Apr. 2022.

[6] D. Seita, P. Florence, J. Tompson, *et al.*, "Learning to Rearrange Deformable Cables, Fabrics, and Bags with Goal-Conditioned Transporter Networks," in *IEEE ICRA 2021*, May 2021, pp. 4568–4575.

[7] M. Lepert, J. Fang, and J. Bohg, *Phantom: Training Robots Without Robots Using Only Human Videos*, arXiv:2503.00779 [cs], Mar. 2025. DOI: 10.48550/arXiv.2503.00779. [Online]. Available: http://arxiv.org/abs/2503.00779 (visited on 03/08/2025).

[8] H. Zhang, J. Ichnowski, D. Seita, J. Wang, H. Huang, and K. Goldberg, "Robots of the Lost Arc: Self-Supervised Learning to Dynamically Manipulate Fixed-Endpoint Cables," in *IEEE ICRA 2021*, May 2021, pp. 4560–4567.

[9] M. C. Nah, A. Krotov, M. Russo, D. Sternad, and N. Hogan, "Learning to manipulate a whip with simple primitive actions – A simulation study," *iScience*, vol. 26, no. 8, p. 107 395, Aug. 2023.

[10] R. Nayeem, S. Bazzi, M. Sadeghi, N. Hogan, and D. Sternad, "Preparing to move: Setting initial conditions to simplify interactions with complex objects," *PLOS Computational Biology*, vol. 17, no. 12, e1009597, Dec. 2021.

[11] M. Edraki, R. Lokesh, A. Krotov, A. Ramezani, and D. Sternad, "Human-Inspired Control of a Whip: Preparatory Movements Improve Hitting a Target," in *2024 10th IEEE RAS/EMBS International Conference for Biomedical Robotics and Biomechatronics (BioRob)*, Sep. 2024, pp. 270–275.

[12] T. Flash and N. Hogan, "The coordination of arm movements: An experimentally confirmed mathematical model," *J. Neuroscience*, vol. 5, no. 7, pp. 1688–1703, Jul. 1985.